Physics – Uspekhi 47 (4) 359 – 370 (2004)

REVIEWS OF TOPICAL PROBLEMS PACS numbers: 28.52.Cx, **52.57.–z**

Feasibility of spherical fusion target compression under two-beam laser irradiation

V B Rozanov

DOI: 10.1070/PU2004v047n04ABEH001741

Contents

Abstract. **The results of investigations of the laser radiation interaction with low-density foamy materials are presented. When such materials are used as the energy absorber in spherical targets with thermonuclear fuel in the laser-driven fusion (LF) problem, the physics of energy absorption and transfer in these media permits a significant reduction of the number of irradiating laser beams (down to two beams) in the implementation of spherical target compression. Traditional irradiation (direct and indirect) schemes involve the use of a large number (100 – 200) of irradiating beams, which is extremely difficult to realize in a fusion reactor.**

1. Introduction

The fundamental problem that must be solved for the demonstration of controlled nuclear fusion involving inertial confinement is the compression stability of a spherical target capsule containing thermonuclear fuel. This requires providing the conditions of target heating whereby the energy input nonuniformity is within several percent (1 – 5%). So stringent a requirement stems from the fact that the compressed-target parameters required for the demonstration of controlled fusion reaction are attained upon a 15 – 45-fold radial capsule compression (by the volume factor $3 \times 10^3 - 10^5$ [1]).

In this formulation, the problem of target compression approaches the problem of energy cumulation [2] but does not coincide with it. In problems of energy cumulation, the external conditions are limited (for instance, the amplitude of a converging spherical shock wave is finite at some distance from the center), but infinite quantities arise at the center (the pressure $p \to \infty$). In problems of target compression with ideal symmetry, limited external conditions result in high yet finite values of the physical quantities (pressure and temperature) in the central domain.

The values of ‘ideal’ quantities are determined by the entropy introduced into the central domain of the target at the heating stage. The similarity of these two problems consists in the fact that both the cumulation limitations (according to E I Zababakhin’s assumption in Ref. [2]) and the lowering of ‘ideal’ quantities as the target is compressed are related to the development of hydrodynamic instability. It is valid to say that to every kind of cumulation there corresponds an instability type.

In the problem of LF target compression, there is an instance of employing the cumulation ideas. Nuckolls et al. [3] considered the compression of a spherical target (a small ball of deuterium – tritium ice) by converging spherical sound waves such that all successive waves arrive at the target center simultaneously with the first wave. To accomplish this, the conditions at the target surface, for instance the laser radiation flux q, should vary in time according to the law (profiled pulse compression)

$$q \propto \left(\frac{1}{1 - t/t_0}\right)^{3\gamma/(\gamma+1)},$$

where t_0 is the pulse duration and the arrival time of the first wave and γ is the adiabatic constant of the material.

It is significant that the pressure, including the high pressure produced at the end of the pulse (of the order 10^{11} atm, formally $p \to \infty$) is weak relative to the target already compressed, and therefore the target is compressed by the sound waves with a minimal increase in the target entropy throughout the process. An analysis of this example of cumulation in Ref. [4] confirms E I Zababakhin’s assumption of cumulation instability, in this case with respect to small deviations from the ideal pulse shape. Despite the infeasibility of this kind of energy cumulation, the idea of laser pulse tailoring has retained its significance in LF as a way of improving the target characteristics under ‘ideal’ (symmetric) conditions.

V B Rozanov P N Lebedev Physics Institute,
Russian Academy of Sciences,
Leninskiĭ prosp. 53, 119991 Moscow, Russian Federation
Tel./Fax (7-095) 132 11 96
E-mail: rozanov@sci.lebedev.ru

Received 18 September 2003, revised 18 December 2003
Uspekhi Fizicheskikh Nauk **174** (4) 371 – 382 (2004)
Translated by E N Ragozin; edited by A M Semikhatov

Table 1. Existing high-power laser facilities and those under construction.

NIF, USA	3ω, 1.8 MJ, 192 beams, indirect compression, full-scale experiments planned for 2008
LMJ, France	3ω, 2 MJ, 240 beams, indirect compression, 2010
Omega, USA	$1\omega - 3\omega$, 60 kJ, direct compression, in service
Iskra-6, Russian Federal Nuclear Center – All-Russian Scientific Research Institute of Experimental Physics, Russia	$1\omega - \omega$, 300 kJ, being designed; the 'Luch'' module: four channels, 12 – 25 kJ, 2003

In the cumulation and compression problems under discussion, the lower the initial perturbations, the higher the energy densities. That is why the task of elucidating the initial perturbation spectrum (including the amplitudes and composition of the modes) is one of the central problems in the physics of target compression.

Two main directions [1] are presently being pursued in the solution to this problem in LF (see Fig. 1).[1] One of them involves the symmetric direct irradiation of a traditionally designed shell target by a large number (several dozen) of laser beam.s. The highest-power facility constructed for solving this problem (the 'Omega' facility, Laboratory for Laser Energetics of Rochester University, USA) has 60 beams. To ensure a uniform energy distribution over the laser beams area and exclude interference effects, special optical devices were introduced into the system (phase plates, a system for spectrum broadening and spectral smoothing, etc.). Direct-compression targets necessitate the conversion of Nd-laser radiation to its third harmonic (to increase the fraction of absorbed energy).

The other direction ('indirect compression') relies on the conversion of laser radiation into the flux of thermal X-ray radiation. An indirect-compression target consists of a massive outer shell — a cylindrically shaped converter — and a spherical capsule with thermonuclear fuel dispensed inside it.

We note that the thermonuclear capsule employed for direct and indirect compression, which contains a set of spherical shells, including a layer of a deuterium – tritium mixture in the form of ice, was proposed in the Lebedev Physics Institute (FIAN) [8, 9] early in the 1970s. At present, it is a universally accepted target design investigated in experiments.

We return to the problem of indirect compression. The laser radiation enters the converter through its entrance holes incident on its inner surface, is absorbed, and produces the plasma, which radiates in the X-ray range. The emission spectrum is rather complicated, but on the average it is close to the thermal one and can be characterized by a temperature of 0.15 – 0.35 keV. The X-ray radiation fills the internal converter cavity and is incident on the capsule surface to cause the ablation of the material of the outer shell and the capsule compression. The difference from direct compression consists in the fact that the X-ray photons penetrate the plasma deeper than the laser radiation photons and give rise to a higher ablation rate, which increases the compression rate.

The indirect compression scheme also requires converting the laser radiation frequency into the third harmonic in order to raise the X-ray radiation yield. The poor energy balance related to the small capsule-to-converter surface area ratio (1 : 5) impels us to employ a higher target compression ($V/V_0 \simeq 10^5$), and therefore the requirements on irradiation uniformity are more stringent in this scheme than for direct compression. The facility most elaborated for the implementation of this direction is the National Ignition Facility (NIF) of the Lawrence Livermore National Laboratory, USA. It employs 192 beams, which enter the target converter in the form of three cones on both sides.

The following fact characterizes the complexity of the irradiation uniformity problem: at the early stage of the laser pulse (prior to the formation of a relatively extensive plasma), each focal region on the internal converter surface irradiated by laser radiation (192 regions!) becomes a source of nonequilibrium (nonthermal) radiation corresponding to the transitions in the *M*-shell of gold (the converter material). This radiation produces 192 nonuniform spots (a peculiar imprint) on the capsule surface, because the converter–capsule distance is different for different spots. This effect may prove to be of crucial importance in the 40-fold radial target compression.

The problems under discussion are schematically represented in Fig. 1. Under compression, the capsule radius varies with time in a similar manner in the versions with direct and indirect irradiation. The spatial density distributions at different time instants (Fig. 1a) are also close. In the case of direct laser irradiation, the laser beam, which is nonuniform due to its partial coherence, is incident on the spherically symmetric density and temperature distributions around the capsule, which are the goal of 'good' compression. The energy of a single laser beam is released in some domain resembling a lens shown in Fig. 1b. The lens boundaries are determined by the position of the critical density surface. The energy release for multiple-beam irradiation is the sum of such 'lenses', provided it is sufficiently uniform. Otherwise, a torch-like plasma flow emerges in the lens region, with the consequential change in the position of the energy release region. Such summation of individual beam contributions determines the requisite number of irradiation directions.

The diagram that illustrates indirect compression depicts one of the three cones along which the laser beams enter the converter (Fig. 1c). Finally, Fig. 1d illustrates that it is in principle possible to precisely focus the beams in the experimental facility. However, complying with all focusing requirements for a multibeam laser is extremely unlikely in a future laser fusion reactor operating with a repetition rate of several hertz and ballistic target delivery to the focus of the laser beams. A laser reactor and target allowing only two or several (6, 8, 12) irradiation directions will offer great advantages, because one of the requirements for the reactor chamber design is the minimization of the number of channels that pierce the chamber blanket. These circumstances underlie the interest in the problem specified by the title of our review.

Table 1 lists high-power laser facilities [10 – 13] that have been constructed or are being constructed,[2] which allow

[1] Additional information and references to earlier papers, along with Ref. [1], can be found in Refs [5 – 7].

[2] We cite the most recent papers because they give the best idea of the conditions and parameters of the facilities.

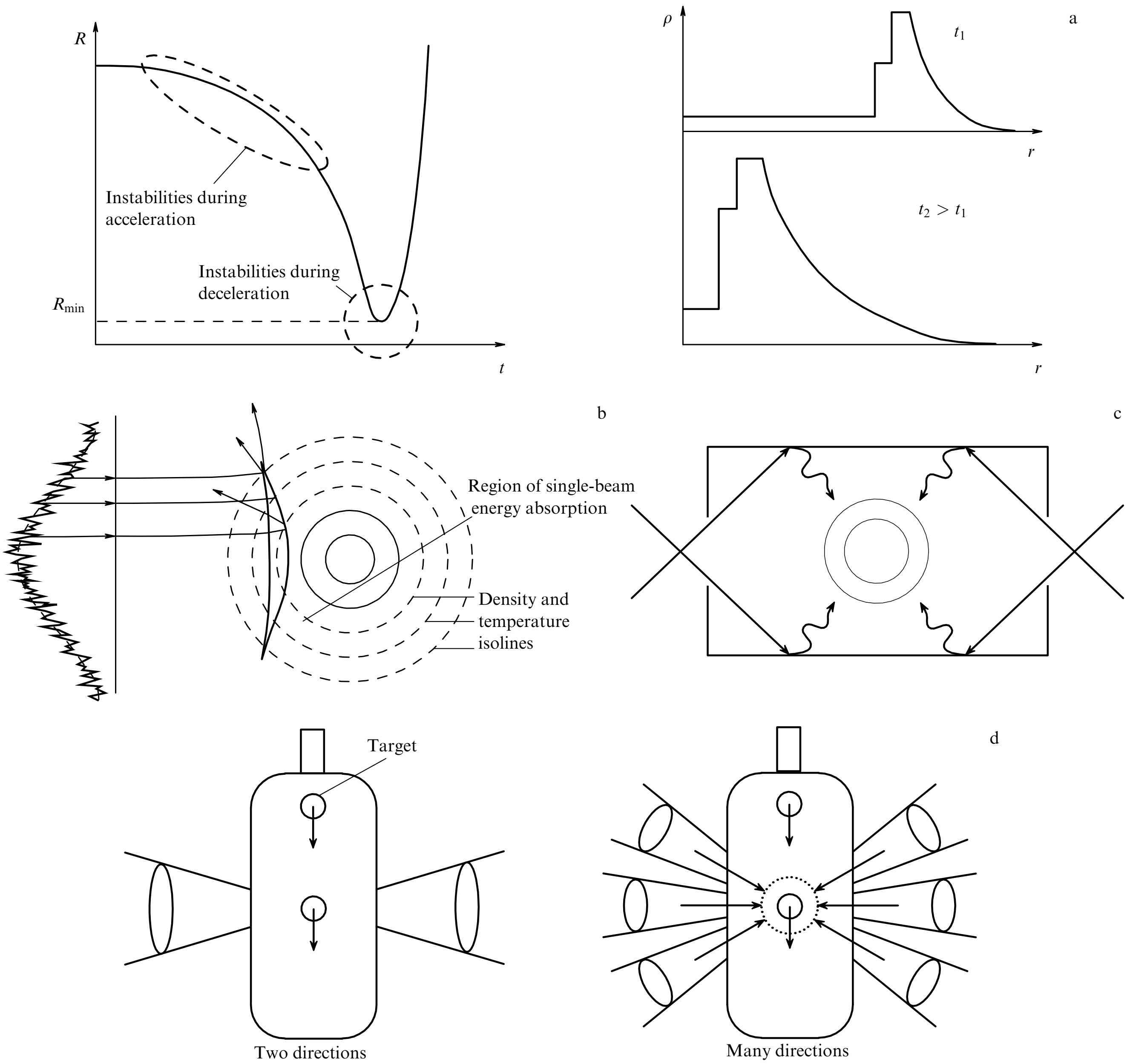

Figure 1. Direct and indirect target irradiation and compression: (a) variation of the target radius with time and radial dependence of the density at the time instants t_1 and t_2; (b) the region of single-beam energy absorption for direct irradiation; (c) indirect compression; (d) the problem of multiple irradiation directions in a laser fusion reactor.

estimating the prospects and parameters of large-scale experiments on compression.

Target irradiation experiments with two or even one beam were staged in the USA in 1974 (KMS Fusion [14] and LANL [15]). In the experiments described in Ref. [14], two mirrors of special (elliptical) shape and two beams were employed to provide a nearly spherical symmetry of irradiation. The beams were focused with short-focus lenses and introduced through the holes at the centers of the mirrors nearest to the beams. Subsequently, they were focused onto the target with a second mirror, which ensured a nearly spherical irradiation symmetry.

The results of experiments on single-beam irradiation of a target, which was made up of a gas-filled sphere and a disk located on the irradiation-free side, were described in Ref. [15]. The sphere shell possessed a profiled thickening on the side under irradiation to compensate for excessive pressure. The disk made it possible to transport a small amount of energy to the irradiation-free side of the target as well. A prepulse (3 J, 10% of the total energy) produced plasma around the target and was favorable to a more uniform heating.

The experiments in Refs [14, 15] were intended to demonstrate compression, which was extremely important at that time. With the laser radiation energy of several dozen Joules, it was possible to achieve 250- and 100-fold volume compressions, which is many times smaller than is required according to present views. The above irradiation schemes were not intended to attain the conditions for fusion ignition and burning, and subsequently they were not elaborated.

2. Physical basis for the feasibility of employing a small number of irradiation directions maintaining spherical symmetry of compression

The LF research of the late 1980s saw the mastering of the technology for producing low-density structured materials with a density of 0.05 – 0.001 g cm^{-3}, which are structurally foamy (polystyrene foam, aerogels) or fibrous (agar). Layers and spherical shells of a given thickness were fabricated of materials with a density close to the critical density for the laser radiation of a specific frequency (1ω — 0.003 g cm^{-3}, 3ω — 0.03 g cm^{-3} for an Nd laser). The absorption of laser radiation and energy transfer in such a medium are significantly different from those in a homogeneous medium. It is precisely the employment of these materials for the absorption of laser radiation in LF targets that is the physical basis of spherically symmetric compression for a small number of irradiation directions.

The target design intended to realize these possibilities was proposed in the Laser-Driven Fusion Department of the Quantum Radiophysics Division of the Lebedev Physics Institute in Refs [16, 17]. The subsequent experimental investigations and numerical simulation of the processes in the targets were pursued with the participation of the Department of Target Technology of the Lebedev Physics Institute (technology development and target fabrication for experiments), TRINITI and RFNC – VNIIEF[3] of the Atomic Energy Ministry of the Russian Federation, the Laser Laboratory of the ENEA Research Center, Frascati, Italy (experimental investigations [18 – 22, 26]), and the Institute of Mathematical Modeling (IMM) of the Russian Academy of Sciences (RAS) (numerical calculations and simulation [23 – 25, 32]). Later in this section, we briefly consider the results of experimental and theoretical investigations and formulate the model of physical processes in a low-density structured medium.

Figures 2a and 2b show photographs of the samples of such media, taken from Refs [18, 23, 24] and made with an electron microscope: one can clearly see the surfaces and cells in the polystyrene foam as well as the surfaces and fibers in the case of agar. When a foamy target is exposed to laser radiation, the radiation is absorbed in the region located along the ray, the depth of the absorption region depending on the target density. Figures 2c and 2d show X-ray photographs of the targets and the density dependence of the absorption depth derived from experiments.

We note that the model of physical processes in a structured plasma, which is discussed at the end of this section, predicts this dependence rather well. Figures 2e – 2g illustrate an important fact: for an oblique incidence of laser radiation and a low target density, the energy is absorbed along the laser beam, subsequently producing a pressure gradient and accelerating the plate (the target shell) along the normal to the surface.

The main results of the experiments in Refs [18 – 22] are as follows:

- the absorption of laser radiation in the structured plasma amounts to 80 – 100% and depends only slightly on the angle of laser radiation incidence;
- there is no regular reflection and refraction of laser radiation; the scattered radiation amounts to 3 – 5% of the incident energy;
- the energy losses related to plasma expansion towards the beam do not exceed 5%;
- the absorption of laser radiation occurs along the laser beam direction and is inherently volume-distributed; the absorption depth in a supercritical-density plasma is given by

$$L \approx \frac{3}{2}\,\pi^2 \left(\frac{\rho_s}{\rho_p}\right)^{1/2} b_0\,,$$

where ρ_s is the density of solid elements, ρ_p is the average plasma density, and b_0 is a small size ('the wall thickness'); the size of large target structures is 5 – 150 μm for different values of ρ_p;
- the pressure in the plasma is equal to several megabars and the energy transfer rate is $(2-4)\times 10^7$ cm s^{-1} for the radiation intensity $(0.5-5)\times 10^{14}$ W cm^{-2};
- the so-called 'greenhouse' effect is observed: during the first 3 – 5 ns, the porous substance accumulates energy with hardly any expansion, which is followed by a nearly isotropic thermal explosion.

It is believed that the above results depend only slightly on the radiation wavelength. The experimental data under discussion were obtained for $\lambda = 1.06$ μm; the absorbed energy fraction measured for $\lambda = 0.53$ μm was close to 100% [26].

Proceeding from experimental data and the results of numerical simulations, one can conceive the following picture of laser radiation absorption in a porous medium. The porous substance is initially, for several dozen picoseconds, transparent for the radiation being absorbed and the radiation penetrates it to some depth. Next, there occur the expansion of solid elements, the collision of plasma streams, and the filling of the pores. The plasma bunches fulfil the function of peculiar 'blackbodies', in which absorption amounts to 100% owing to multiple reflections by randomly located dense fragments. This may also account for the absence of regular reflection and refraction. The depth of the laser radiation penetration into the porous target observed in experiments is formed at this stage.

Due to expansion of the solid elements of the material and collisions of plasma streams, long-lived stochastic density oscillations may exist in the plasma. As a result, a part of the plasma can have a density close to the critical one or even below it. In these regions, the energy of laser radiation is absorbed through the inverse Bremsstrahlung and resonance mechanisms. We consider the processes that may exert an effect on the duration of the oscillations and estimate the corresponding quantities.

The lifetime of dense structures produced due to the expansion of solid elements and the collisions of plasma streams is limited by the ion viscosity

$$\eta \simeq \frac{v^2 \tau_{ii}}{3}\,,$$

where

$$\tau_{ii} = 1.1 \times 10^{-13}\,\frac{(AT_i)^{3/2}}{\rho Z^4}$$

[3] TRINITI — the Troitsk Institute for Innovation and Thermonuclear Research; RFNC – VNIIEF — the Russian Federal Nuclear Center – All-Russia Scientific Research Institute of Experimental Physics.

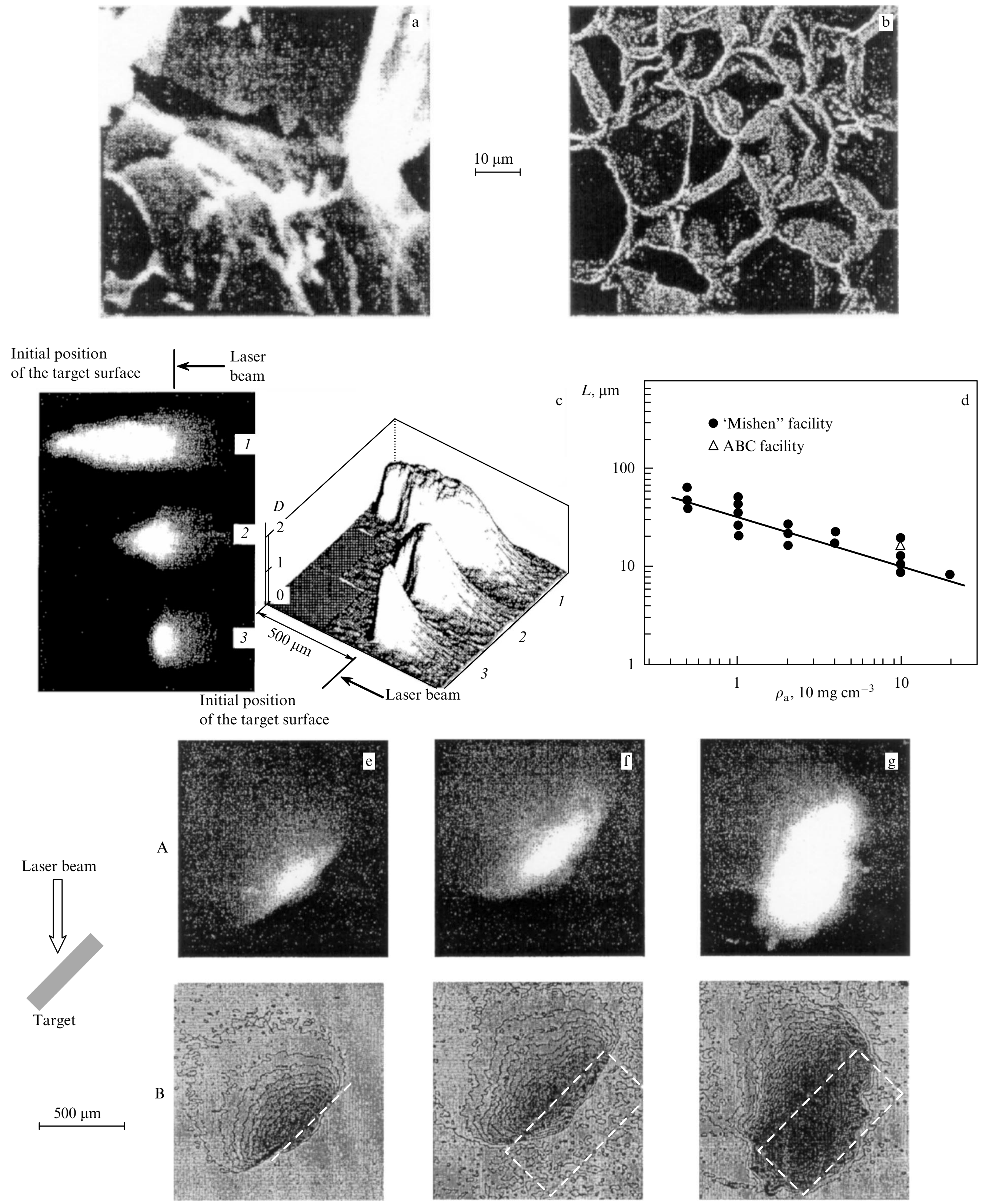

Figure 2. Results of experimental investigations: (a) agar structure; (b) cellular polystyrene structure; (c) X-ray photographs of targets of different densities (*1* — 1 mg cm^{-3}, *2* — 4 mg cm^{-3}, *3* — mylar film, 1.4 g cm^{-3}); (d) absorption depth as a function of the average density of the porous medium; (e) – (g) X-ray pinhole camera images of the experiments with oblique incidence of laser radiation (A) and result (B) of their processing [(e) mylar film, $d = 7$ μm; (f) agar, 5 mg cm^{-3}, $d = 400$ μm; (g) agar, 2 mg cm^{-3}, $d = 400$ μm; the dashed line shows the initial target position].

is the ionic collision time, A and Z are the atomic number and charge of plasma ions, respectively, $T_{\rm i}$ is the ion temperature (keV), v is the characteristic ion velocity, and ρ is the plasma density (in g cm^{-3}). In a carbon plasma with the temperature

1 keV and the electron density 10^{21} cm^{-3}, structures of size $x \simeq 30$ μm may exist for a time $t = x^2/(2\eta) = 1-2$ ns and of size $x \simeq 100$ μm for 15 – 20 ns.

The stream collisions inside the pores generate a succession of shock waves. The shock front thickness is determined by the ion path and the Mach number, which may be close to unity in a hot plasma, i.e., the shock front thickness may be equal to about 5 – 20 μm, and the density becomes almost uniform after one or two collisions (in 1 – 2 ns). We note that the density may rise several-fold in these collisions in comparison with the average one [in strong shock waves, by the factor $(\gamma+1)/(\gamma-1)$, where γ is the adiabatic constant]. All this may lead to the formation of reduced-density regions characterized by a larger penetration depth for the laser radiation and a stronger absorption (owing to a greater entanglement of the trajectories of laser radiation in the plasma volume). The assumption that these regions exist is indirectly confirmed by experiments [20].

A role may be played by the fact that a significant part of the solid elements in a real three-dimensional porous structure that find themselves in the absorption region are initially either not irradiated by the incident radiation at all (owing to the screening by the overlying elements) or irradiated at angles of laser radiation incidence close to $\pi/2$. In a cubic structure with thin plane walls, for instance, about 5/6 of the total mass is initially not irradiated when the radiation is normally incident on one of the faces. In view of this effect, it can be hypothesized that as the irradiated solid elements expand, they produce a plasma with the average density several times lower than the average density of the medium. The streams of this plasma collide with each other and with irradiation-free (cold) elements to produce oscillations with an amplitude high enough for the formation of subcritical-density plasma regions.

It is likely that the process outlined above is responsible for the aforementioned 'greenhouse effect': the porous substance retains its initial volume until the radiation energy transferred to the irradiated elements is distributed over the entire mass that finds itself in the absorption region and until the oscillations die out. This stage may be estimated to last for several (3 – 5) oscillations, which agrees well with experimental results. We note that such oscillations have so far escaped direct observation.

Using the RAPID code, which involves combined solution of one-dimensional equations of fluid dynamics and Maxwell equations for the description of laser radiation, a series of one-dimensional calculations was performed to simulate the laser irradiation of an inhomogeneous medium consisting of a sequence of thin polystyrene layers (CH composition). The simulations were performed for two structure types — with coarse and fine meshes. The former was modeled with a system of layers of with the thickness $\Delta x = 1$ μm and spacing $L = 49$ μm, and the latter with a system of layers with $\Delta x = 0.1$ μm and $L = 4.9$ μm. The average density of both media was $\rho = 2 \times 10^{-2}$ g cm^{-3}.

The numerical simulation was performed for a radiation pulse at the third-harmonic frequency of an Nd laser, the total length of the laser pulse was 2.5 ns, the peak intensity I_{max} was $(0{,}2-2) \times 10^{15}$ W cm^{-2}. The factor β in the thermal conductivity coefficient was an additional parameter: $\beta > 1$ corresponds to the Spitzer value $\varkappa_0$ and $\beta = 0.01$ to the suppression of thermal conduction $\varkappa = \varkappa_0/100$. The results of simulation for the average energy transfer rate u are summarized in Table 2. Simulations showed that as many as 10 density oscillations may occur. The ion viscosity does not lead to an appreciable oscillation damping for 1 – 3 ns if the size of dense regions is 10 – 30 μm.

Table 2. Results of 1-D layered-system burning-through simulations.

Absorber structure	I_{max}, 10^{14} W cm^{-2}	β	u, 10^7 cm s^{-1}
Coarse cell	2.0	> 1	2.0
	2.0	0.01	1.5
	20	> 1	5.1
	20	0,01	3.5
Fine cell	2.0	> 1	3.0
Homogeneous medium	2.0	> 1	3.5
	20	> 1	8.0

Figure 3a shows the spatial distributions of the velocity, the density, and the temperature in the two aforementioned cases of Spitzer thermal conductivity, a coarse cell and a low flux, plus a fine mesh and a low flux.

The processes observed in experiments and simulations and the nonequilibrium state of the resultant plasma are indicative of the necessity of 'constructing' an effective equation of state for the structured medium in which the formation of pressure at different points of a cell occurs after the instant of energy input. The time delay depends on the position of the observation point inside the pore, the pore size L, and the sound velocity c_s. This time can be estimated as $\tau = nL/c_s$, where n is the number of oscillations. The value is $\tau \simeq 0.3$ ns for $L = 30$ μm, and $\tau \simeq 0.05$ ns for $L = 5$ μm, i.e., the medium with finer pores is closer to the continuous medium in properties. The same is true of the electron thermal conduction, which may be suppressed when the material is strongly inhomogeneous, while at a later stage it is close to that of Spitzer.

The relevant model of the effective equation of state of the foam is based on the following considerations. The heating and evaporation of the solid elements of the porous medium in response to laser radiation absorption occurs rather rapidly, and therefore the internal electron energy can be defined by the ideal-gas expression

$$\varepsilon_e = \frac{3}{2} \frac{Z}{m_i} kT_e ,$$

where m_i is the substance ion mass, T_e is the electron temperature, and Z is the ion multiplicity, which can be taken equal to the atomic number because light elements are almost fully ionized for $I \simeq 10^{14} - 10^{15}$ W cm^{-2}. In this case, $\varepsilon_e \simeq E/M$, where E is the absorbed energy and M is the mass of the heated material. But the one-dimensional calculations performed with the DIANA code show that the electron pressure is nonuniformly distributed on the cell scale and the cell-averaged pressure p_e is much lower than the pressure in the vaporized mass of a solid element:

$$p_e < \frac{Z}{m_i} \rho kT_e .$$

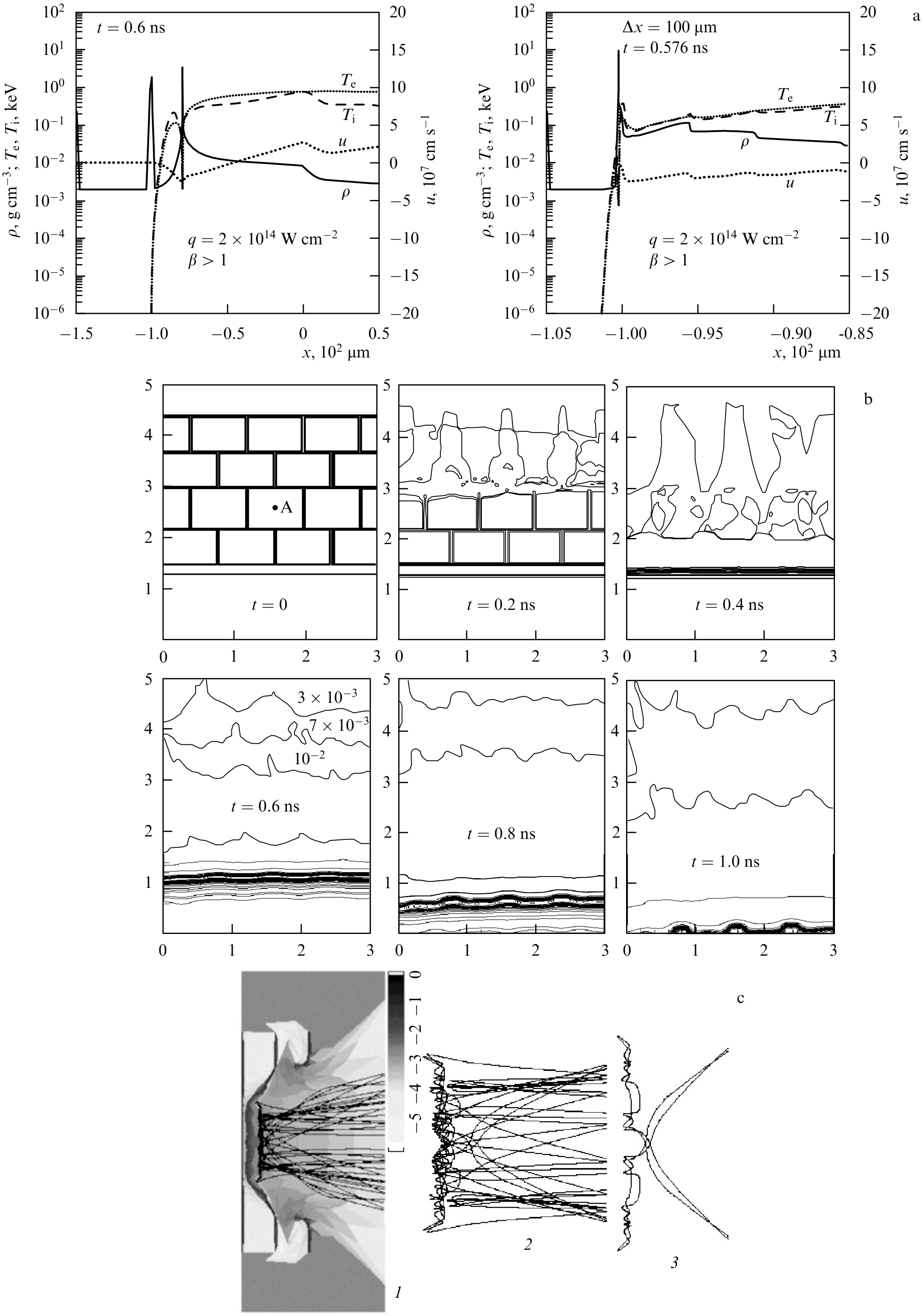

Figure 3. Results of numerical simulations: (a) one-dimensional simulation of the laser irradiation of a layered system with the Spitzer thermal conductivity for coarse cells and a low intensity (at the left) and for fine cells and a low intensity (at the right); (b) density isolines (g cm^{-3}) in the 'brick' foam model at different time instants; (c) instant of the second impact in the layered system (*1* — density distribution and ray trajectories, *2* — ray trajectories, *3* — trajectories of two pairs of the peripheral rays of the beam).

We introduce an effective temperature $T_{\rm eff} = \alpha T_e$, where the parameter $\alpha < 1$ is time-dependent ($\alpha \to 1$ on the expiry of the homogenization time, which amounts to several nanoseconds in the case under consideration).

Then,

$$p_{\mathrm{e}} = \frac{Z}{m_{\mathrm{i}}}\,\rho k T_{\mathrm{eff}} = \alpha\,\frac{Z}{m_{\mathrm{i}}}\,\rho k T_{\mathrm{e}}\,.$$

To determine T_{eff} (or the α parameter), we use the simplest relaxation equations

$$\frac{\mathrm{d}T_{\mathrm{eff}}}{\mathrm{d}t} = \frac{T_{\mathrm{e}} - T_{\mathrm{eff}}}{\tau}\,, \qquad \frac{\mathrm{d}\alpha}{\mathrm{d}t} = \frac{1-\alpha}{\tau} - \alpha\,\frac{\mathrm{d}\ln T_{\mathrm{e}}}{\mathrm{d}t}\,, \tag{1}$$

where $\tau = nL/c_{\mathrm{s}}$ is the time delay introduced above. The isothermal sound velocity

$$c_{\mathrm{s}} = \left(\frac{Z}{m_{\mathrm{i}}}\,kT_{\mathrm{e}}\right)^{1/2}$$

was used in the above model. The number n is a fitting parameter in this model, but the value $n = 3-5$ obtained from the one-dimensional simulations of laser irradiation of the layered medium was found to provide a reasonable description of experimental data.

To model two-dimensional effects, simulations were made for a stratified inhomogeneous medium in a cylindrical geometry. Figure 3b depicts the target prior to irradiation ($t = 0$), the diaphragms are disks and rings. The vertical distance between the disks is 70 μm and 80 μm between the rings, the diaphragm thickness is 3 μm, the material (CH) density in the diaphragms is 0.1 g cm^{-3}, the gas density in the cavities is 10^{-5} g cm^{-3}, and the average density of the medium is 7×10^{-3} g cm^{-3}. Located beneath is a 20-μm thick normal-density CH layer to imitate the capsule shell. The laser radiation parameters are as follows: $\lambda = 1.06$ μm, the sectional intensity distribution

$$I(r) = I_0 \exp\left(-\frac{r^2}{R_{\mathrm{b}}^2}\right)$$

(the beam radius $R_{\mathrm{b}} = 300$ μm); for $r > R_{\mathrm{b}}$, the intensity $I = 0$ and the beam energy is 850 J, i.e., the average intensity is $\bar{q} \simeq 3 \times 10^{14}$ W cm^{-2}; the pulse has the form of an isosceles triangle with a total duration of 1 ns. Figure 3b shows the density field evolution at the time instants $t = 0$, 0.2, 0.4, 0.6, 0.8, and 1 ns.

The calculation performed shows that the plasma is essentially nonequilibrium for more than half the pulse duration: the behavior of the electron temperature is qualitatively different from the behavior of the pressure and the ion temperature. Therefore, the effective relaxation-type equation can be treated as some approximation of the real processes, because it describes the delay of pressure formation, but not its oscillations. The latter are significant in providing the answer to the question of compression stability of the entire target.

The results in Fig. 3 allow the conclusion that an intermediate layer of a volume-structured material reduces the effect of large-scale irradiation nonuniformities. At a later stage, one can clearly see the imprint (shape perturbations of the accelerated layer caused by external action) produced by the absorber layers immediately adjacent to the capsule. This process is controllable, for instance, by applying a two-layer absorber with the pore size decreasing with depth.

An important but yet unsolved task in the hydrodynamic instability problem is determination of the perturbation spectrum made up of large-scale perturbations related to the number of irradiation beams, small-scale perturbations arising from the beam structure, and the perturbations caused by pressure oscillations in the foam. The structure of the foamy absorber then smoothes out the perturbations of all scales.

For a system consisting of three parallel polyethylene (CH) layers, we outline a two-dimensional burning-through simulation performed by A Caruso and C Strangio with the COBRAN code in the ENEA Laboratory (Frascati). The parameters of the simulation were as follows: the layer thickness $d = 0.5$ μm; the layer separation ('the pore size') was 75 μm (the average density 6.7 mg cm^{-3}); $\lambda = 1.054$ μm; a triangular-shaped laser pulse with the energy 40 J (the pulse emerged at $t = 0$, reached its peak at $t = 0.7$ ns, and terminated at $t = 2$ ns); and the focal spot diameter was 240 μm (the focal point was located at $z = 450$ μm, while the front layer of the system was situated at $z = 0$, the z axis coinciding with the laser beam axis). First of all, it is pertinent to note that as shown by the simulation of a one-layer system, the time t_{b} that it takes for one layer to become transparent exceeds the time t_{s} it takes for a nonevaporated part of the layer to travel a distance equal to the characteristic pore dimension: $t_{\mathrm{b}} = 1.37$ ns, $t_{\mathrm{s}} = 0.85$ ns. This implies that there occurs a 'snow plow'-type motion in the system of layers, with the effect that the mass of the accelerated nonevaporated part increases as collisions occur.

Of greatest interest is the instant of the second impact ($t \simeq 0.9$ ns). Figure 3c shows the density map with ray trajectories, the total set of calculated trajectories, and two pairs of the most extreme of them. One can see that the trajectory distribution undergoes a qualitative change in comparison with that in the case of conventional burning through plane foils and goes over to 'entanglement' (a part of the peripheral rays is deflected to the center of the spot, while a part of the central ones goes to the periphery). This may have a bearing on smoothing of irradiation nonuniformities. It is noteworthy that the reflected flux of laser radiation is practically suppressed by that time, i.e., the absorption efficiency increases.

To conclude this section, we emphasize once again that the theoretical notions, on the one hand, and experiments, on the other, are in satisfactory agreement as regards the main parameters, such as the average plasma temperature and pressure, the energy transfer rate, the absorption depth and the absorbed energy fraction, the time of substantial plasma expansion, and several others. The oscillations of physical quantities in the plasma related to homogenization of the initial target structure are an important characteristic of in-target processes, and they manifest themselves in experiments only indirectly. It would be of interest and significance to directly observe the oscillations. The statistical nature of absorption ensures a certain degree of its independence from the external conditions (the angle of laser radiation incidence, the wavelength of laser radiation, the intensity).

As a result, the model where the laser radiation is absorbed in the plasma along a ray with the absorption depth corresponding to Fig. 2 (and the formula in Section 2) and the equation of state of the relaxation type can be accepted in the subsequent target simulation.

3. Target design and symmetry of the absorbed energy distribution

The proposed model of laser radiation absorption in low-density structured materials describes the volume radiation

Table 3. Results of one-dimensional simulations of target compression and burn.

Target type	CD capsule, 2.6 kJ	DT gas, 100 kJ	DT ice, 100 kJ	DT ice, 2.1 MJ
t_c, ns	0.497	1.54	3.50	5.89
η, %		7.22	9.73	4.72
ρR_{fuel}, g cm^{-2}	0.09	0.0523	0.190	0.38
$\bar{T}_{\mathrm{fuel}}$, keV	3.1	12	7.88	3.71
G		0.1	1.04	7.93
N_{DD}	10^{10}			

Notation: t_c — compression time, η — fraction of laser energy converted to the kinetic energy of the shell, ρR_{fuel} — optical thickness of compressed fuel, $\bar{T}_{\mathrm{fuel}}$ — average temperature of compressed fuel, G — fusion gain coefficient, N_{DD} — DD-neutron fusion yield.

absorption in a layer of certain thickness. In this section, we present the target designs that make the 'best' use of this model. Specifically, these designs ensure a neutron yield in the fusion burn under perfectly symmetric conditions, an acceptable symmetry of the absorbed energy distribution under irradiation by a small number of beams, and a low sensitivity to parameters that may presently prove to be defined with an insufficient accuracy (for instance, the absorption layer thickness or the form of energy distribution in the beam).

The target designs for a laser pulse energy E_{L} of 2.1 MJ, 100 kJ, and 2.6 kJ are given in Fig. 4a.[4] The energy E_{L} is selected such that its highest value ensures the energy gain $G \simeq 8$, i.e., intense fusion burn. The threshold conditions ($G \simeq 0.1-1$) are achieved for 100 kJ. And, lastly, the lowest value $E_{\mathrm{L}} = 2.6$ kJ is selected in such a way as to achieve an appreciable neutron yield when the target is exposed to two beams.

Because the absorption depth depends on the absorber density, in a broad range of E_{L} values it is possible to select a thickness such that the ratio of the external absorber radius (where absorption occur) to the capsule radius (where ablation and shell acceleration occur) remains within the range $2-1.2/1$. This corresponds to a good energy balance in the target and the transfer of a significant fraction (5–8%) of laser energy to the deuterium–tritium (DT) fuel. The results of one-dimensional simulations of these targets are collected in Table 3.

The simulations given in Table 3 were performed in the IMM, RAS, with the DIANA code, which solved the standard LF set of equations describing the absorption of laser radiation, ablation, the target compression and burn, and the substance properties [27]. A recently published report [28] describes the results of experiments on the compression of targets with the DD gas at the Omega facility (USA, see Table 1) under conditions of good irradiation symmetry.

The results of calculations with the DIANA code and the experimental data in Ref. [28] for a rectangular laser pulse are in satisfactory agreement, as is evident from the data in Table 4. The notation in Table 4 is the same as in Table 3: T_{i} is the temperature averaged over the DD-gas mass during the burn time (it was determined in the simulations that the neutron yield arose from the inner part of the DD gas corresponding to 30% of the total value of $\langle \rho R \rangle$). The data

Table 4. Correspondence of the data of simulations and experiments on target compression.

	E_{L}, kJ	τ_{L}, ns	t_c, ns	N_{DD}, 10^{11}	$\langle \rho R \rangle$, mg cm^{-2}	T_{i}, keV
[26]	23.3	1		1.27	61	3.6
Diana	23.3	1	1.5	1.5	43	3.2

given suggest that the results predicted on the basis of the DIANA code for targets with a foamy absorber ('greenhouse-type' targets) for a good symmetry of absorbed energy distribution may be justified experimentally and are of interest in subsequent applications.

We next consider the question of symmetry of absorbed laser energy distribution for a small number of irradiation beams. The absorption of laser radiation in our model occurs in a layer whose thickness L is small or comparable to the target radius R. The angular distribution of power release density $\sigma(\theta, \varphi)$ is given by the formula

$$\sigma(\theta, \varphi) = \int_{R-L}^{R} \dot{\varepsilon}(r, \theta, \varphi) r^2 \,\mathrm{d}r\,, \qquad \dot{\varepsilon} = \sum_{i=1}^{N} \dot{\varepsilon}_i\big(r, \psi_i(\theta, \varphi)\big)\,. \quad (2)$$

Here, i corresponds to a given beam ($1 \leqslant i \leqslant N$), R is the target radius, r, θ, and φ are the coordinates of a point in a small volume in the sphere (where the energy is absorbed), $\psi_i(\theta, \varphi)$ is the angle between the ith beam axis and the radius vector of a point selected, and $\dot{\varepsilon}$ is the absorption rate per unit volume. As the layer thickness $L \to 0$, formula (2) becomes a relation describing the irradiance of the target surface.

Therefore, as follows from the model in Section 2, using a foamy layer for the absorption of laser radiation bridges the gap between the problem of obtaining a uniform absorbed energy distribution and the problem of obtaining a uniform irradiance. For a finite number of beams, the problem of obtaining a uniform irradiance has an exact solution, which consists of the following. When the beam diameter is equal to the target diameter, the intensity distribution in the beam is given by

$$I(r) = I_0 \left(1 - \frac{r^2}{R^2}\right)^{1/2}$$

(where r is the distance to the beam axis and R is the radius of the target and the beam) and the surface distribution of the beams belongs to one of the classes found in a relatively recent paper [29], then perfect symmetry is achieved for an even number of beams, beginning with $N = 6$. To obtain perfect symmetry, use can also be made of the number of beams $N = 8$, 12, 20 and their different combinations (for instance, 14, 20, or 60). The symmetry of the arrangement of $N = 6$, 8, 12, and 20 beams corresponds to the symmetry of perfect crystals. The results in Ref. [29] were used in finding the number of beams ($N = 60$) and their spatial arrangement for the Omega laser facility (USA).

For targets with a foamy material absorber, the effect of real energy distribution in the beam (which is Gaussian rather than proportional to $(1 - r^2/R^2)^{1/2}$, as in Ref. [29]), of different models and versions of laser radiation absorption depth [the layer thickness L in formula (2)], of the beam-to-target diameter ratio, of the variation of target size with time owing to heating and expansion, and of several other factors must be examined in the context of this approach. These issues were elucidated in a series of numerical calculations whose results were given in Refs [23–25].

[4] Targets with a foamy absorber can be given the common title 'greenhouse-type' targets (GHTs) [16, 17].

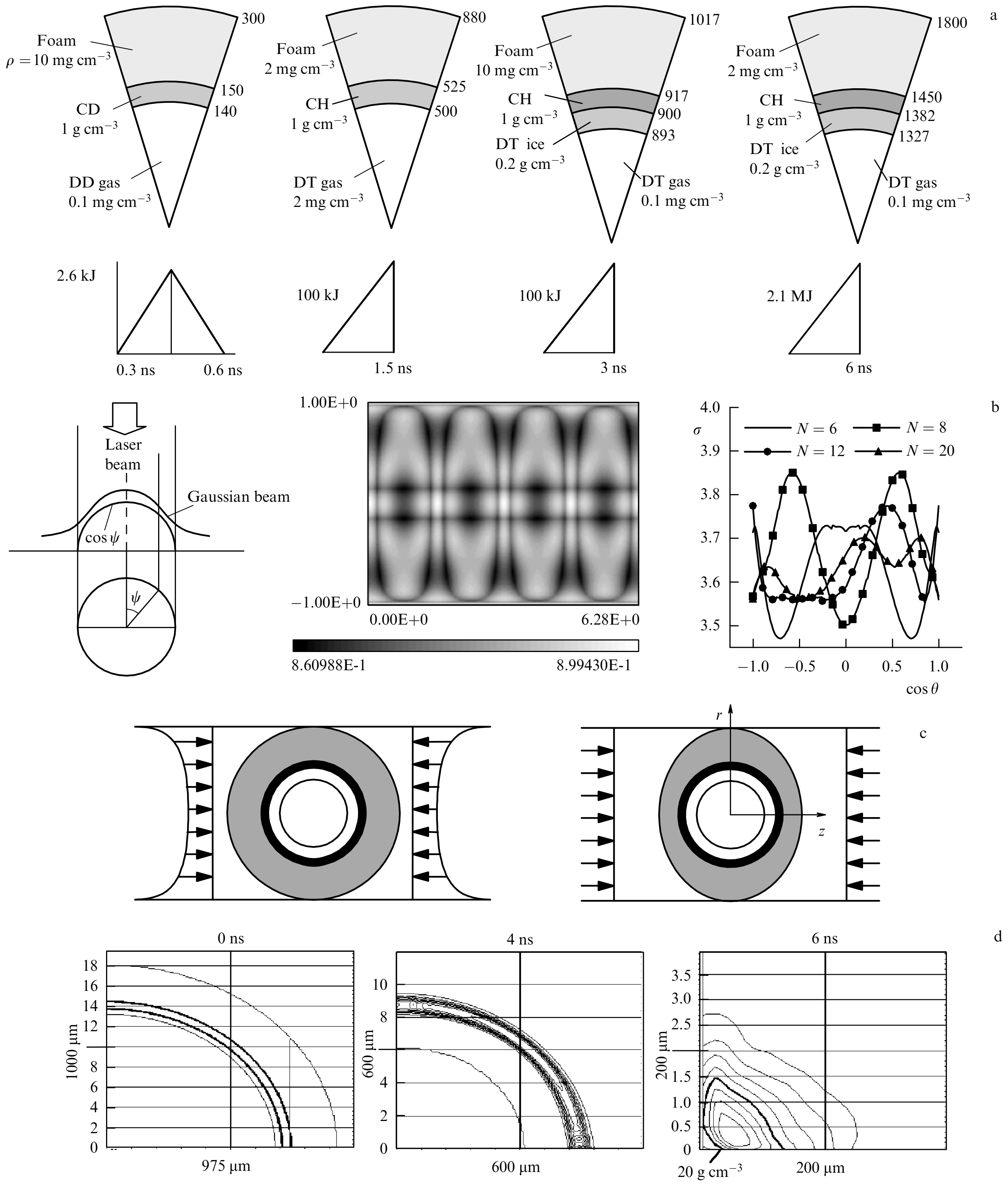

Figure 4. (a) Target designs for different energies of the laser pulse. (b) Map of σ for mass-uniform absorption ($L = 0.3R$, sections of the field σ for different versions of the beam distribution). (c) Schematic of two-beam irradiation and formulation of the problem of a profiled absorber. (d) Two-dimensional two-beam compression simulations with the reference FIAN profile for three time instants.

The main results of the calculations are given in Fig. 4. Figure 4b depicts the profiles of energy distribution in the beam from Ref. [29] and the Gaussian beam (not to scale), as well as the definition of the angle ψ_i in formula (2); an example of the map of the $\sigma(\theta, \varphi)$ distribution for $N = 6$ and the mass-uniform absorption with $L = 0.3R$; and the dependences $\sigma(\theta, \varphi_i)$ for $N = 6$, 8, 12, and 20 for the meridians φ_i passing through the beam axis (these meridians do not coincide for different N). In these calculations, the index of skewness $\zeta = (\sigma_{\max} - \sigma_{\min})/(\sigma_{\max} + \sigma_{\min})$ varied within the limits 2 – 4%, the greatest perturbations corresponding to the low harmonics of spherical functions, i.e., to long-wavelength perturbations with $n = 6$ and $n = 8$, which grow slowly during compression. The results depend only slightly on the relation between L and R and the target R and beam R_b radii for $R_b > R$. However, the index of skewness significantly rises when the beam radius is smaller than the target radius.

Further development of the approach underlying formula (2) (the uniformity of absorbed energy is proportional to the uniformity of irradiance) lies in the potentiality of employing only two beams for the irradiation. (This possibility was first discussed in the joint paper of the Quantum Radiophysics Division of FIAN and the IMM presented at the XXVII Zvenigorod Conference on Plasma Physics in 2000.) Indeed, it is easy to show that the beam energy distribution profile of the form

$$I(r) = \frac{I_0}{\cos\phi} = \frac{I_0}{(1 - r^2/R^2)^{1/2}}$$

(an 'anti'-[29] profile in a sense) formally produces a perfectly symmetric irradiance of the sphere with only two counter-propagating beams (Fig. 4c). Furthermore, it is possible to find the beam profile for the attainment of the absorbed energy distribution close to the spherically symmetric one for different R and L (the results are presented in Refs [23 – 25, 32]).

The intensity increase at the beam edge (formally infinite in the irradiation problem) may present a problem in the realization of two-beam irradiation, and therefore a study was made of the possibility of using beams with a uniform intensity. In this case, the uniform absorbed energy distribution $\sigma(\theta, \varphi)$ is achieved through selection of the proper absorber shape. This form was determined (it is qualitatively shown in Fig. 4c). We believe that combining the potentialities of a profiled beam (of the $I_0/\cos\phi$ type, but not necessarily coinciding with it) with those of a profiled absorber (Fig. 4c) makes it realistic to attains a uniform absorbed energy distribution in the target and ensure its spherically symmetric subsequent compression for reasonable requirements for the laser and the target.

Therefore, the solution to the problem specified in the title of our review becomes feasible. Naturally, the Gaussian distribution versions for $N = 6$, 8, 12, etc. retain their attractiveness, but there emerge new design possibilities. The beams may be divided into groups and focused in accordance with the target size taking its compression into account and with the onset of laser irradiation in each group of the beams at the appropriate time instant. These versions of irradiation are possible for different N [25].

The symmetry and uniformity of the absorbed energy distribution are an intermediate result. More critical is the compression process and the target shape prior to ignition and fusion burn. This issue was investigated with the aid of two-dimensional compression simulations [30]. For a two-beam irradiation, the anticipated difficulty is related to the fact that the absorption zone in the polar region (on the beam axis) is large (the energy density is low), while the absorption zone near the target equator (at the periphery of the beam) is narrow (the energy density is high). However, the energy transfer in the absorber equalizes the conditions; as a result, preliminary simulations of compression [21, 25] suggest that the target symmetry can be retained under two-beam compression for a rather long period of time. Figure 4d gives an idea of the symmetry of the process for the 2.1-MJ target, the proximity to one-dimensional calculations being retained even late in the process ($t = 5 - 6$ ns).

The results on the problem of symmetry and uniformity of the absorbed energy distribution can be summarized as follows. For targets with a foamy absorber, the initial perturbation spectrum consists of low-order mode perturbations associated with the number of irradiation beams, of the perturbations arising from beam nonuniformities (interference effects), and of the perturbations arising from the influence of foamy absorber structure and the effects of smoothing the nonuniformities related to the energy transfer in the absorber. The possibility of fabricating absorber foams with cells of different sizes gives grounds to select favorable conditions for the two last-named processes. In the context of the models considered, the low-order mode perturbations turn out to be at an acceptable level (Fig. 4b). Determining the contribution of medium-range modes, including those associated with the beam structure, invites further experimental investigation.

We make two remarks to conclude the section concerned with the targets. A target specimen for the two-beam irradiation with an energy of 2.6 kJ was fabricated in FIAN [24], and hence an experiment on the two-beam irradiation on the existing facilities and those under construction appears to be possible.

A comparison of the calculated 2.1-MJ target parameters given in Table 3 with the calculated NIF target parameters [31] was made in Refs [21, 24]. While the values of laser energy and thermonuclear target yield are close (17.6 MJ for the NIF, 15.5 MJ for the GHT), we note that the NIF target effects a 'cooler' and stronger compression: prior to the onset of burn, the DT-region energy is 17.5 kJ, the minimal radius of this region is 44 μm, and the degree of radial compression is $C = 22$. Similar results were obtained for the GHT: 122 kJ, 98 μm, $C = 14$. The NIF target data are more arduous and are therefore more susceptible to the action of hydrodynamic instabilities, with the target compressed by the irradiation along 192 directions. The GHT compression can be effected along six or eight directions, and it is not improbable that only two directions would turn out to be sufficient.

4. Conclusion

The prospect of achieving good compression symmetry for a target with a foamy absorber (of the 'laser greenhouse' type) irradiated by a small number of laser beams relies on the fact that the volume-distributed absorption in the foam retains the features inherent in the problem of irradiance, for which the formal possibility of constructing a spherically symmetric distribution has already been proven. The physical models of the processes and the mathematical codes for calculating different stages of target irradiation, compression, and burn make it basically possible to seek optimal parameter values for different specific experimental conditions. The results obtained and their development with subsequent experiments taken into account will permit the energy reactor design to be substantially simplified, because the concept under discussion allows a radical reduction in the number of irradiation directions and an alleviation of requirements on the mutual coherence of the beams, their profiling, and supposedly the radiation wavelength.

The works on the problem under discussion were performed in the TRINITI, the IMM of the RAS, and the

Quantum Radiophysics Division of FIAN and supported by the Russian Foundation for Basic Research (Grant Nos 01-02-17361, 01-02-17336, 02-02-16966) and the INTAS (Grant No. 0572).

References

1. Rozanov V B et al., in *Energy from Inertial Fusion* (Ed. W J Hogan) (Vienna: IAEA, 1995) Ch. II, p. 21
2. Zababakhin E I *Usp. Fiz. Nauk* **85** 721 (1965) [*Sov. Phys. Usp.* **8** 295 (1965)]
3. Nuckolls J et al. *Nature* **239** 139 (1972)
4. Afanas'ev Yu V et al. *Prikl. Mat. Mekh.* **39** 451 (1975) [*J. Appl. Math. Mech.* **39** 427 (1975)]
5. Basov N G (Ed.) *Teoriya Nagreva i Szhatiya Nizkoentropiĭnykh Termoyadernykh Misheneĭ* (Theory of Heating and Compression of Low-Entropy Fusion Targets) (Tr. Fiz. Inst. Akad. Nauk SSSR, Vol. 134) (Moscow: Nauka, 1982)
6. Rozanov V B *Kvantovaya Elektron.* **24** 1095 (1997) [*Quantum Electron.* **27** 1063 (1997)]
7. Lindl J *Phys. Plasmas* **2** 3933 (1995)
8. Afanas'ev Yu V et al. *Pis'ma Zh. Eksp. Teor. Fiz.* **21** 150 (1975) [*JETP Lett.* **21** 68 (1975)]
9. Afanas'ev Yu V et al., in *IAEA 5th Conf. Proc., Tokyo, Japan, 11–15 Nov. 1974* Vol. 2 (Vienna: IAEA, 1975) p. 559
10. Tarter C B, in *Inertial Fusion Sciences and Applications 2001, IFSA2001*: *Proc. of the 2nd Intern. Conf., Kyoto, Japan, Sept. 9–14, 2001* (Eds K A Tanaka, D D Meyerhofer, J Meyer-ter-Vehn) (Paris: Elsevier, 2002) p. 9
11. Galmiche D, Cherfils C, in *ECLIM2002*: *27th European Conf. on Laser Interaction with Matter, 7–11 October 2002, Moscow, Russia* (Proc. SPIE, Vol. 5228, Eds O N Krokhin, S Y Gus'kov, Yu A Merkul'ev) (Bellingham, Wash.: SPIE, 2003) p. 28
12. Regan S P et al., in *Inertial Fusion Sciences and Applications 2001, IFSA2001*: *Proc. of the 2nd Intern. Conf., Kyoto, Japan, Sept. 9–14, 2001* (Eds K A Tanaka, D D Meyerhofer, J Meyer-ter-Vehn) (Paris: Elsevier, 2002) p. 89
13. Rukavishnikov N N et al., in *ECLIM2002*: *27th European Conf. on Laser Interaction with Matter, 7–11 October 2002, Moscow, Russia* (Proc. SPIE, Vol. 5228, Eds O N Krokhin, S Y Gus'kov, Yu A Merkul'ev) (Bellingham, Wash.: SPIE, 2003) p. 665
14. Gomberg H *Laser Focus* (December) 18 (1974)
15. McCall G H, Morse R L *Laser Focus* (December) 40 (1974)
16. Gus'kov S Yu, Rozanov V B, in *Vseros. Konf. po Fizike Plazmy i Upravlyaemomu Termoyadernomu Sintezu, Zvenigorod, 1994*: *Annotatsii Dokladov* (All-Russia Conf. on Plasma Phys. and Controlled Nuclear Fusion, Zvenigorod, 1994: Abstracts of Papers)
17. Gus'kov S Yu, Zmitrenko N V, Rozanov V B *Zh. Eksp. Teor. Fiz.* **108** 548 (1995) [*JETP* **81** 296 (1995)]
18. Bugrov A É et al. *Zh. Eksp. Teor. Fiz.* **111** 903 (1997) [*JETP* **84** 497 (1997)]
19. Bugrov A É et al. *Zh. Eksp. Teor. Fiz.* **115** 805 (1999) [*JETP* **88** 441 (1999)]
20. Gus'kov S Yu et al. *Kvantovaya Elektron.* **30** 191 (2000) [*Quantum Electron.* **30** 191 (2000)]
21. Vergunova G A et al., Preprint No. 58 (Moscow: Lebedev Physics Institute, Russian Academy of Sciences, 1999)
22. Bugrov A E et al., in *ECLIM2002*: *27th European Conf. on Laser Interaction with Matter, 7–11 October 2002, Moscow, Russia* (Proc. SPIE, Vol. 5228, Eds O N Krokhin, S Y Gus'kov, Yu A Merkul'ev) (Bellingham, Wash.: SPIE, 2003) p. 8
23. Stepanov R V et al., in *ECLIM2002*: *27th European Conf. on Laser Interaction with Matter, 7–11 October 2002, Moscow, Russia* (Proc. SPIE, Vol. 5228, Eds O N Krokhin, S Y Gus'kov, Yu A Merkul'ev) (Bellingham, Wash.: SPIE, 2003) p. 233
24. Rozanov V B et al., in *Inertial Fusion Sciences and Applications 2001, IFSA2001*: *Proc. of the 2nd Intern. Conf., Kyoto, Japan, Sept. 9–14, 2001* (Eds K A Tanaka, D D Meyerhofer, J Meyer-ter-Vehn) (Paris: Elsevier, 2002) p. 200
25. Gus'kov S Yu et al. *Kvantovaya Elektron.* **33** 95 (2003) [*Quantum Electron.* **33** 95 (2003)]
26. Gus'kov S Yu et al. *Pis'ma Zh. Eksp. Teor. Fiz.* **64** 462 (1996) [*JETP Lett.* **64** 502 (1996)]
27. Samarskiĭ A A et al. *Vopr. At. Nauki Tekh. Ser. Metodika Programmy Chislennogo Resheniya Zadach Matem. Fiz.* (2(13)) 38 (1983)
28. *LLE Review Quaterly Report* **93** (October–November) 1 (2002); http://www.lle.rochester.edu/pub/review/v93/93_Review.pdf
29. Simmons W W, in *Solid State Lasers for Application to Inertial Confinement Fusion* (*ICF*) (Proc. SPIE, Vol. 2633, Ed. W F Krupke) (Bellingham, Wash.: SPIE, 1995) p. 249
30. Iskakov A B et al., Preprint No. 48 (Moscow: Lebedev Physics Institute, Russian Academy of Sciences, 2000)
31. Haan S W et al. *Phys. Plasmas* **2** 2480 (1995)
32. Rozanov V B et al., Preprint No. 23 (Moscow: Lebedev Physics Institute, Russian Academy of Sciences, 2002)